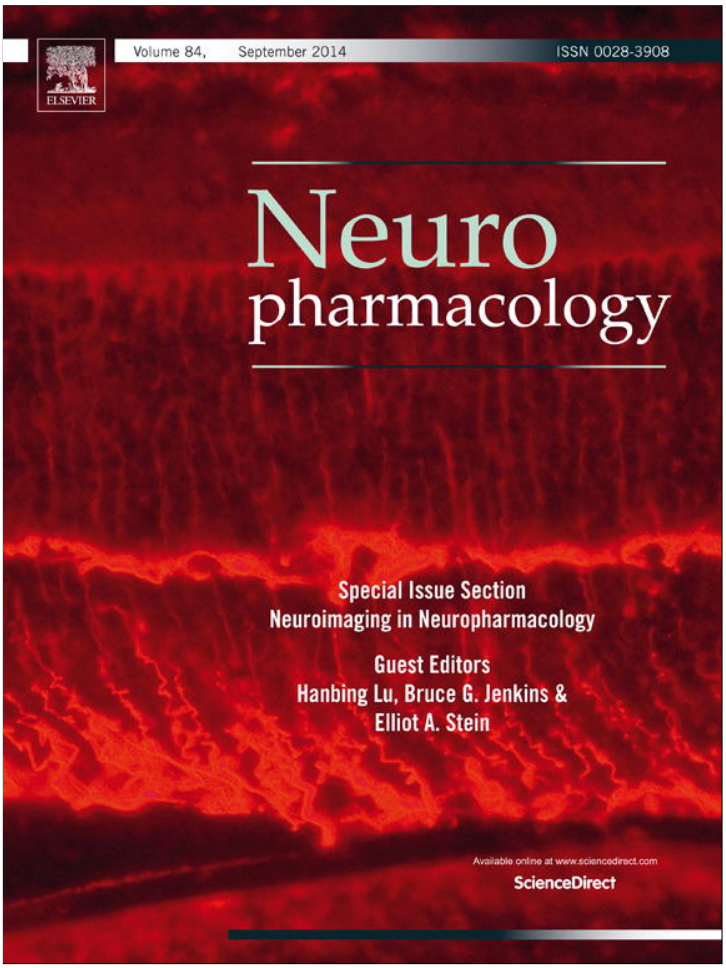

Neuropharmacology 84 (2014) 152–158

Contents lists available at ScienceDirect

Neuropharmacology

journal homepage: www.elsevier.com/locate/neuropharm

Evaluation of P-glycoprotein (abcb1a/b) modulation of [^{18}F]fallypride in MicroPET imaging studies

Markus Piel [a,*,1], Ulrich Schmitt [b,1], Nicole Bausbacher [c], Hans-Georg Buchholz [c], Gerhard Gründer [d], Christoph Hiemke [b], Frank Rösch [a]

[a] Institute of Nuclear Chemistry, Johannes Gutenberg-University, Fritz-Strassmann-Weg 2, D-55128 Mainz, Germany
[b] Department of Psychiatry and Psychotherapy, University Medical Center of the Johannes Gutenberg-University, Mainz, Germany
[c] Department of Nuclear Medicine, University Medical Center of the Johannes Gutenberg-University, Mainz, Germany
[d] Department of Psychiatry and Psychotherapy, RWTH Aachen University, Aachen, Germany

ARTICLE INFO

Article history:
Received 29 June 2012
Received in revised form
25 March 2013
Accepted 29 April 2013
Available online 29 August 2013

Keywords:
[^{18}F]fallypride
Dopamine D_2/D_3 receptors
P-Glycoprotein
Cyclosporine A
Positron emission tomography

ABSTRACT

[^{18}F]Fallypride ([^{18}F]FP) is an important and routinely used D_2/D_3 antagonist for quantitative imaging of dopaminergic neurotransmission *in vivo*. Recently it was shown that the brain uptake of the structurally related [^{11}C]raclopride is modulated by P-glycoprotein (P-gp), an important efflux transporter at the blood–brain barrier. The purpose of this study was to determine whether the brain uptake of [^{18}F]FP is influenced by P-gp. For examination of this possible modulation microPET studies were performed in a rat and a mouse model. Hence, [^{18}F]FP was applied to Sprague Dawley rats, half of them being treated with the P-gp inhibitor cyclosporine A (CsA). In a second experimental series the tracer was applied to three different groups of FVB/N mice: wild type, P-gp double knockout (abcb1a/1b (−/−)) and CsA-treated mice. In CsA-treated Sprague Dawley rats [^{18}F]FP showed an elevated standard uptake value in the striatum compared to the control animals. In FVB/N mice a similar effect was observed, showing an increasing uptake from wild type to CsA-treated and double knockout mice. Since genetically or pharmacologically induced reduction of P-gp activity increased the uptake of [^{18}F]FP markedly, we conclude that [^{18}F]FP is indeed a substrate of P-gp and that the efflux pump modulates its brain uptake. This effect – if true for humans – may have particular impact on clinical studies using [^{18}F]FP for assessment of $D_{2/3}$ receptor occupancy by antipsychotic drugs.

This article is part of the Special Issue Section entitled 'Neuroimaging in Neuropharmacology'.

1. Introduction

The ability of xenobiotics to cross the blood–brain barrier (BBB) is generally influenced by the physicochemical properties of the compound, such as molecular weight, hydrogen bond donors and acceptors and/or lipophilicity. Furthermore, the uptake of xenobiotics into the central nervous system (CNS) can also be restricted by a number of drug metabolizing enzymes and efflux transporters, located at the BBB (Dutheil et al., 2009; Pardridge, 2007). P-glycoprotein (P-gp), localized at the luminal side of the endothelial cells of the BBB, is one of these transport proteins and acts as an active efflux pump for a wide range of compounds. In former studies it was shown that P-gp has a protective physiological function in the BBB by preventing the entrance of neurotoxic substances into the CNS (Bartels et al., 2008; Ohtsuki and Terasaki, 2007).

P-gp, which is encoded by the multidrug resistance 1 gene in humans (MDR1/ABCB1), is a member of the highly conserved superfamily of ATP-binding cassette (ABC) transport proteins and uses the hydrolysis of adenosine triphosphate (ATP) to enable this transport against concentration gradients. P-gp consists of 12 highly hydrophobic transmembrane helices, organized in two

Abbreviations: BP_{ND}, non-displaceable binding potential; CsA, cyclosporine A; CYP3A4, cytochrome P_{450} 3A4; DVR, distribution volume ratio; [^{18}F]FP, [^{18}F]Fallypride; MDR1/ABCB1, multidrug resistance 1 gene in humans; OSEM2D, 2-dimensional ordered-subset expectation maximization iterations; P-gp, P-Glycoprotein; PET, positron emission tomography; ROI, region of interest; SPECT, single photon emission computed tomography; SRTM, simplified reference tissue model; SUV, standard uptake value; TAC, time activity curve.

* Corresponding author. Tel.: +49 6131 3925701; fax: +49 6131 3926606.
E-mail addresses: piel@uni-mainz.de (M. Piel), ulrich.schmitt@unimedizin-mainz.de (U. Schmitt), Nicole.Bausbacher@unimedizin-mainz.de (N. Bausbacher), buchholz@nuklear.klinik.uni-mainz.de (H.-G. Buchholz), ggruender@ukaachen.de (G. Gründer), hiemke@uni-mainz.de (C. Hiemke), frank.roesch@uni-mainz.de (F. Rösch).

[1] Contributed equally to this work.

0028-3908/$ – see front matter © 2013 Elsevier Ltd. All rights reserved.
http://dx.doi.org/10.1016/j.neuropharm.2013.04.062

groups of six helices linked by very polar extracellular linker regions, and two intracellular nucleotide binding domains responsible for the ATP binding (Aller et al., 2009). Due to the broad range of structurally unrelated compounds that can interact with P-gp, the presence of several binding sites was assumed, which resulted in the characterization of four different binding sites for substrates and modulators (Aller et al., 2009; Martin et al., 2000).

The importance of P-gp for the therapeutic effect of drugs has become evident in the 1970s, when it was shown that P-gp is responsible for the resistance of cancer cells against some chemotherapeutics (Juliano and Ling, 1976). Subsequently in the 1980s, P-gp was found to be a part of the BBB and thus regulating the uptake of several drugs into the CNS (Cordon-Cardo et al., 1989). Therefore, a large number of studies were performed to examine the mechanisms of interaction between different drugs and P-gp and the influence on the pharmacokinetic profile and the pharmacodynamic activity of the drug.

Furthermore, the clinical efficacy of drugs which are P-gp substrates is additionally modulated by polymorphisms in the ABCB1 gene (Bozina et al., 2008). Hence, not only the properties of the drug, but also genetic variants in the treated subjects account for a successful therapy (Uhr et al., 2008).

Since PET and SPECT are essential methods for molecular imaging of neurotransmission *in vivo*, it is of crucial importance to identify whether the established radiotracers are substrates of P-gp. If this is the case, it results in a reduced brain uptake of the compound and requires an additional kinetic parameter, for example for the determination of receptor density or availability, respectively. Consequently, a number of PET studies were performed recently to evaluate possible interactions between radiotracers and P-gp (Colabufo et al., 2010; Elsinga et al., 2005). So far, [^{18}F]fallypride ([^{18}F]FP), a clinically used high affinity D_2-like antagonist (Mukherjee et al., 1995; Siessmeier et al., 2005), was not examined *in vivo* with regard to a possible interaction with P-gp, although this tracer sometimes shows strongly differing standard uptake values (SUVs) in healthy subjects (Vernaleken et al., 2011). Hence, this behavior could be partly explained by [^{18}F]FP being a substrate of P-gp and the varying SUVs being caused by polymorphisms in the genome of the subjects. The assumption that [^{18}F]FP is a substrate of P-gp is further supported by the fact that [^{11}C]raclopride, a structurally similar D_2-like antagonist, has shown an increased brain uptake *in vivo* by blocking P-gp (Ishiwata et al., 2007). However, in a recent study using a bidirectional transport assay, it was also shown that [^{18}F]FP passage is not modulated by P-gp in this *in vitro* model (Tournier et al., 2011).

Therefore, the purpose of the present study was to investigate possible effects of P-gp on the brain uptake of [^{18}F]FP *in vivo*, by comparing rats and mice with active or inactive P-gp using PET imaging in a microPET-scanner. The inactivation of P-gp was performed using cyclosporine A (CsA) for both rodent models, which has been proven as a potent P-gp modulator in a number of studies. Since CsA also interferes with cytochrome P_{450} 3A4 (CYP3A4), which is an important enzyme for the metabolism of most xenobiotics, it cannot be excluded that this interaction increases the brain uptake of the tracer, too. Hence, a P-gp double knockout model was also examined in the mouse studies, thus avoiding a modulation of the brain uptake by CsA via the CYP3A4 pathway.

2. Experimental/materials and methods

2.1. Radiochemistry

[^{18}F]FP was synthesized via ^{18}F-direct fluorination of the tosylated precursor ((S)-N-[(1-allyl)-2-pyrrolidinyl)-methyl]-5-(3-toluenesulfonyloxy-propyl)-2,3-dimethoxybenzamide using a modified TRACERlab™ FX F-N (GE Healthcare) automated synthesis module. The reaction procedure was performed as described for [^{18}F]desmethoxyfallypride with minor modifications for the formulation of the tracer (Gründer et al., 2003). The precursor (5 mg, 10 mmol) was dissolved in 1 mL acetonitrile and reacted with the dried [^{18}F]fluoride cryptate complex for 20 min at 85 °C. [^{18}F]FP was separated using semi-preparative high-performance liquid chromatography (HPLC). The product containing fraction was diluted with water and passed over a C18 cartridge (SepPak plus C18, Waters). The product was eluted with 1 mL ethanol, the solvent evaporated *in vacuo*, and the tracer redissolved in 2–5 mL of an isotonic sodium chloride solution and sterilized by filtration.

2.2. Animals

Abcb1a/1b (−/−) double knockout mice (P-gp knockout; FVB/N background), wild type controls (also FVB/N) and Sprague Dawley rats were used. Animals had access to food and water *ad libitum*. Temperature and humidity were kept at 24 ± 2 °C and 60%, respectively. All animals were maintained on a 12-h light/12-h dark cycle. Handling occurred only during the light cycle. All animal experiments were performed in accordance with the European Communities Council Directive of 24 November 1986 (86/609/EEC) and the German law for animal welfare and were approved by the local ethical committee for animal experiments.

2.3. In vivo imaging studies in Sprague Dawley rats

MicroPET imaging was performed with a Siemens/Concorde Microsystems microPET Focus 120 small-animal PET camera (Siemens/Concorde, Knoxville, TN, USA). Sprague Dawley rats were anaesthetized with 2.5% isoflurane in medical oxygen, placed in supine position in the small-animal PET scanner and warmed with a heating lamp. After cannulation of the tail vein, a 10 min transmission scan was performed using a ^{57}Co point source. Following an intravenous bolus injection of [^{18}F]FP (28.8 ± 4.5 MBq) to wild type (n = 5, 190–340 g) and cyclosporine A treated rats (n = 5, 210–260 g, CsA 50 mg/kg i.p. 30 min before injection of the tracer), a dynamic emission scan was accomplished for 1 h. The obtained list-mode files were rebinned to sinograms with 19 frames (3 × 20 s, 3 × 60 s, 3 × 120 s, and 10 × 300 s) and reconstructed by four iterations of 2-dimensional ordered-subset expectation maximization iterations (OSEM2D) with scatter and attenuation correction. This finally results in a 128 × 128 × 95 matrix, with 0.87 × 0.87 × 0.80 mm^3 voxels. Reconstructed images were analyzed with the modeling computer software PMOD Base (PBAS, PMOD Technologies Ltd., Zurich, Switzerland). Striatum and cerebellum were chosen as regions of interest (ROIs) and defined on coronal slices based on the stereotaxic rat brain atlas (Paxinos and Watson, 2007). Elliptical regions of interest (ROIs) were drawn on the left and right striata over four slices and on the cerebellum over two slices. The resulting volumes of interest (VOIs) showed a total volume of about 45 μL for the striata, which was in good accordance with values published in the literature and about 35 μL for the cerebellum (Andersson et al., 2002). The radioactivity in the left and right striatum was averaged for each time point to obtain a time activity curve (TAC) for the whole striatum. The TAC for the cerebellum was generated in an analogous manner. Both TACs were decay corrected to the injection time and normalized concerning the injected dose and the weight of the animal to obtain the SUVs [SUV = (radioactivity in Bq per mL/injected radioactivity in Bq) × body weight in g] for each time point.

The kinetic modeling was performed using a pixel-wise kinetic modeling tool (PXMOD, PMOD Technologies Ltd., Zurich, Switzerland), following a slightly modified published procedure (Constantinescu et al., 2011). Hence, in a first step k_2 was estimated using a simplified reference tissue model (SRTM), followed by a calculation of k_2', which then was used to determine the binding potential via a Logan plot with fixed k_2'. The simplified reference tissue model (Gunn et al., 1997) uses the following equation for the modeling:

$$C_T(t) = R_1 C_R(t) + \left\{ k_2 - \frac{R_1 k_2}{1 + \mathrm{BP}} \right\} C_R(t) e^{-\left[\left(\frac{k_2}{1+\mathrm{BP}}\right)+\lambda\right]t} \quad (1)$$

where C_T and C_R are the concentrations in the region of interest and the reference region, R_1 (=K_1/K_1') is the ratio of relative tracer delivery between the region of interest and the reference region, k_2 is the efflux rate constant from the region of interest, λ is the decay constant and ⊗ is the convolution operator. For the fitting of this equation the Gunn BFM simplified reference tissue model with 400 basic functions was chosen, thus giving values for the binding potential BP_{ND}, the efflux constant k_2 and the ratio R_1. Based on the assumption that $K_1'/k_2' = K_1/k_2$ the efflux constant from the reference region k_2' can be calculated from $k_2' = k_2/R_1$.

The determination of the binding potential BP_{ND} was performed using the noninvasive graphical method of Logan (Logan et al., 1996), requiring only a region of interest, a reference region and an average efflux constant from the reference region. This graphical analysis of reversible systems uses the following equation for the calculation:

$$\frac{\int_0^T C_T(t)\mathrm{d}t}{C_T(T)} = \mathrm{DVR}\left[\frac{\int_0^T C_R(t)\mathrm{d}t + C_R(T)/k_2\prime}{C_T(T)}\right] + \mathrm{int}\prime \quad (2)$$

where DVR is the distribution volume ratio, which is the ratio of a distribution volume (DV) in a receptor-rich region to the DV in a receptor-free region, k_2' is the efflux rate constant from the reference region and *int*′ is the intercept. After an equilibration time t^* of the tracer, the DVR can be obtained as slope and *int*′ as intercept from a linear fit of equation (2). Afterward the binding potential (BP_{ND}) was calculated via $BP_{ND} = DVR - 1$. Finally parametric maps of the BP_{ND} with a threshold of 3% were generated, by using the values obtained from the Logan plot.

2.4. In vivo imaging studies in FVB/N mice

FVB/N mice were anaesthetized with ketamine/xylazine by intraperitoneal injection (i.p.; 16 mg/kg xylazine; 120 mg/kg ketamine), placed in supine position in the small-animal PET scanner and warmed with a heating lamp. After cannulation of the mouse tail vein, [^{18}F]FP (4.8 ± 0.5 MBq) was administered intravenously as a bolus injection to wild type (n = 5, 23–45 g), P-gp knockout (n = 5, 26–43 g) and treated animals (n = 5, 22–43 g, CsA 50 mg/kg i.p. 30 min before injection of the tracer), a dynamic emission scan was accomplished for 30 min. The obtained list-mode files were rebinned to sinograms with 13 frames (3 × 20 s, 3 × 60 s, 3 × 120 s, and 4 × 300 s) and reconstructed by four iterations of OSEM2D without scatter and attenuation correction. This finally results in a 256 × 256 × 95 matrix, with 0.43 × 0.43 × 0.80 mm^3 voxels. Reconstructed images were analyzed according to the method described above, choosing striatum and cerebellum as ROIs based on a digital mouse brain atlas. The corresponding VOIs for the striata were generated from 4 slices with a volume of about 13 μL, which was in good accordance with values published in the literature and for the cerebellum from 2 slices giving a volume of about 5 μL (Slow et al., 2003).

2.5. Statistics

Data are given as mean ± standard deviation of the mean (SD). Statistical analysis was performed by t-test for independent variables (GraphPad Prism 4). P-values of ≤0.05 were considered statistically significant.

3. Results

3.1. Radiochemistry

Following the synthesis procedure described above, [^{18}F]FP was produced in a total synthesis time of about 80 min with a radiochemical purity ≥ 97%. The tracer was obtained in radiochemical yields of 35–65%, with an average of 54%, and the specific activities ranged between 200 and 2800 GBq/μmol, with an average of 800 GBq/μmol.

3.2. In vivo imaging studies in Sprague Dawley rats

After bolus injection of [^{18}F]FP to untreated Sprague Dawley rats the tracer showed a fast uptake into the brain and a slow washout (Fig. 1). The striatal tracer levels reached a plateau after 20 min lasting for the remaining measurement with maximum SUVs of about 2.6 g/mL. In the cerebellum the uptake peaked early (<1 min p.i.) reaching a SUV of 2.73 ± 0.27 g/mL, followed by a fast clearance of [^{18}F]FP, resulting in SUVs of 0.28 ± 0.02 and 0.18 ± 0.02 at 30 and 60 min p.i., respectively. Using CsA-treated Sprague Dawley rats, similar uptake kinetics were observed, but CsA-treated animals showed significantly (t = 2.7713, $p \leq 0.05$, Fig. 5) higher striatal SUVs. In the striatum of P-gp blocked animals SUVs of about 3.90 ± 0.23 g/mL were observed between 10 and 60 min p.i., while for the cerebellum values of 0.36 ± 0.09 and 0.26 ± 0.06 at 30 and 60 min p.i. were determined, respectively. Therefore, CsA-treatment resulted in a mean increase of radioactivity levels of about 45% in the striatum and about 48% in the cerebellum from 30 to 60 min p.i., which is clearly visible in normalized SUV images of wild type and CsA-treated animals (Fig. 2).

The kinetic analysis using the simplified reference tissue model resulted in comparable mean values for the BP_{ND}, R_1 and k_2 of 11.03 ± 0.63, 0.704 ± 0.024 and 0.294 ± 0.013 min^{-1} for the wild type and 10.76 ± 0.42, 0.711 ± 0.027 and 0.291 ± 0.010 min^{-1} for the CsA-treated group (Table 1). Furthermore, for both groups the efflux rate constant from the reference region k_2' was calculated using the obtained values of R_1 and k_2. This resulted in mean values for k_2' of 0.416 ± 0.017 min^{-1} for the wild type and 0.412 ± 0.022 min^{-1} for the CsA-treated group.

For the subsequently performed noninvasive graphical Logan analysis a model with a fixed k_2' was chosen, in which the beforehand calculated k_2' values were used as input parameters. In a first attempt the analysis was done by using a maximal relative error criterion for the fitting of the equilibration time t^*. Although very small error limits of 2% were used, this resulted in a relative short t^* of about 15 min in some animals and thus in a lower BP_{ND}. Hence, the fitting procedure was changed and a fixed t^* of 40 min was used, giving comparable binding potentials of 13.65 ± 0.79 and 13.38 ± 0.36 for the wild type and CsA-treated group. The

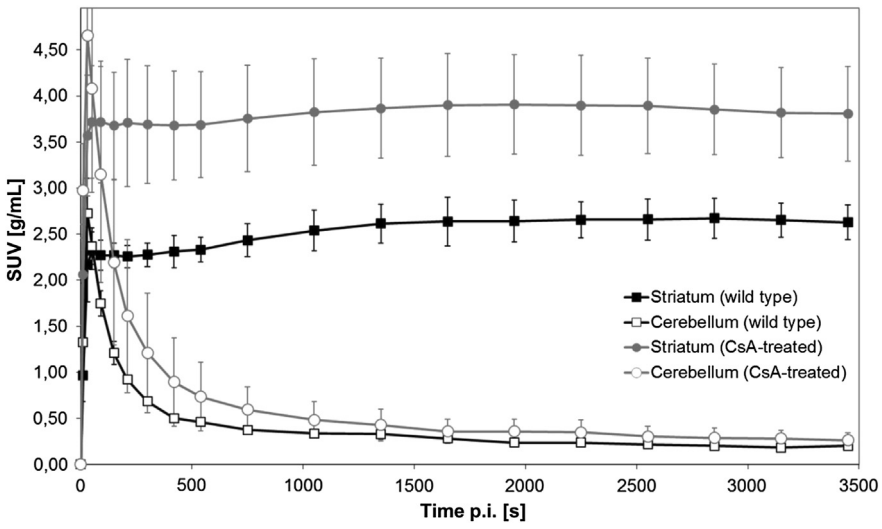

Fig. 1. Time activity curves from microPET-studies of [^{18}F]FP. Curves were drawn from activity measurements in striatum and cerebellum in wild type and CsA-treated Sprague Dawley rats. Each curve gives the mean SUV±SD from 5 animals.

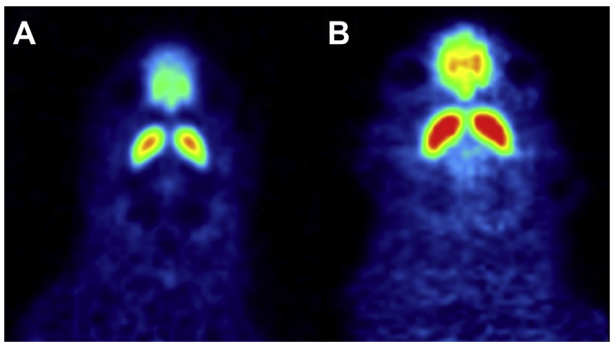

Fig. 2. Color coded uptake images. Coronal slices of the brain uptake of [^{18}F]FP in wild type (A) and CsA-treated (B) Sprague Dawley rats. Uptake is shown as averaged SUV from 40 to 60 min p.i., with a normalized color code (0–3.5 g/mL) for both images.

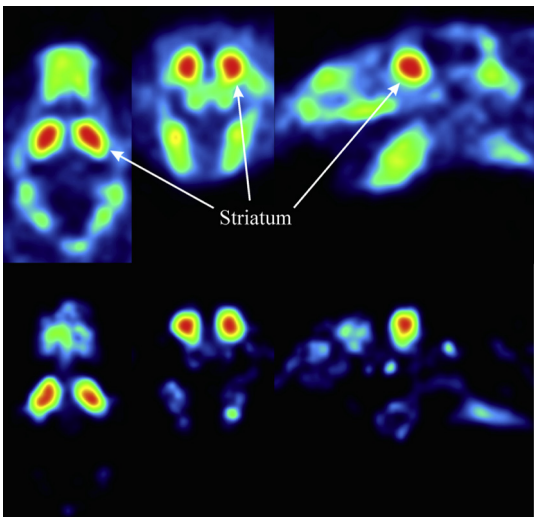

Fig. 3. Color coded uptake images. Representative horizontal, coronal and sagittal brain slices of the brain uptake of [^{18}F]FP in a CsA-treated Sprague Dawley rat. The upper row shows the averaged SUV from 40 to 60 min p.i. (color code: 0–3.5 g/mL), while the lower row shows the corresponding parametric maps of the binding potential BP_{ND} (color code: 0–10, threshold: 3%).

afterward calculated parametric maps of the BP_{ND} demonstrated the high specific binding of [^{18}F]FP in the striatum. Shown in Fig. 3 is a representative comparison of horizontal, coronal and sagittal brain slices of SUV images (upper row) and the corresponding parametric BP_{ND} maps (lower row) of [^{18}F]FP in a CsA-treated Sprague Dawley rat. Besides the specific binding of the [^{18}F]FP in the striatum and the olfactory bulb (upper left image), also the uptake in the skull (upper left image) and jawbone (upper middle and right images), which is caused by metabolism of [^{18}F]FP under release of [^{18}F]fluoride, clearly can be seen.

3.3. *In vivo imaging studies in FVB/N mice*

Time activity curves of the microPET imaging studies in wild type, CsA-treated and double knockout abcb1a/1b (−/−) FVB/N mice are summarized in Fig. 3. Compared to the experimental series in rats, the mouse models revealed slightly different uptake kinetics. Highest SUVs were measured from 40 to 120 s p.i., followed by a brain clearance of the tracer until a stable plateau was reached in the striatum after ~20 min. The double knockout abcb1a/1b (−/−) animals in particular showed a high uptake at the beginning of the measurement followed by a slow brain clearance compared to the CsA-treated and the wild type group.

The highest brain uptake of the tracer was observed in abcb1a/1b (−/−) double knockout mice with a significant difference to either treated ($t = 4.7660$, $p \leq 0.01$) or untreated wild type mice ($t = 6.1392$, $p \leq 0.001$), showing SUVs of 2.29 ± 0.15 g/mL in the striatum and of 0.44 ± 0.05 g/mL in the cerebellum at 30 min p.i.. CsA-treatment of wild type mice resulted also in significantly ($t = 2.8294$, $p \leq 0.05$) higher values compared to untreated wild type mice with SUVs of 1.86 ± 0.18 g/mL in the striatum and of 0.31 ± 0.06 g/mL in the cerebellum, whilst the untreated wild type animals showed SUVs of 1.53 ± 0.11 in the striatum and of 0.24 ± 0.01 in the cerebellum at 30 min p.i. (Fig. 5). Hence, compared to the wild type animals in the double knockout abcb1a/1b (−/−) mice a mean increase in the uptake (15–30 min p.i.) of about 50% and 125% for striatum and cerebellum was found, whilst in the CsA-treated animals an elevated uptake (15–30 min p.i.) of 20% and 35% for striatum and cerebellum was observed (Fig. 5).

Table 1
Results of the kinetic modeling of [^{18}F]FP in Sprague Dawley rats. Shown are the results of both models, the simplified reference tissue model (SRTM) and the noninvasive graphical Logan analysis with fixed k_2', in wild type and CsA-treated Sprague Dawley rats (BP_{ND}: non-displaceable binding potential; R_I: ratio of relative tracer delivery between the region of interest and the reference region; k_2 efflux rate constant from the region of interest; k_2' efflux rate constant from the reference region; *int*′: intercept of the graphical Logan analysis; DVR: distribution volume ratio).

Wild type		Animal 1	Animal 2	Animal 3	Animal 4	Animal 5	Mean ± SEM
SRTM	BP_{ND}	12.88	10.63	8.94	12.32	10.40	11.03 ± 0.63
	R_I	0.754	0.753	0.626	0.661	0.744	0.704 ± 0.024
	k_2 (min^{-1})	0.340	0.295	0.297	0.249	0.288	0.294 ± 0.013
	k_2' (min^{-1})	0.392	0.392	0.474	0.377	0.388	0.416 ± 0.017
Logan	int′	−3326	−3607	−2879	−4610	−3317	−3548 ± 259
	DVR	16.36	14.45	11.69	16.54	14.24	14.65 ± 0.79
	BP_{ND}	15.36	13.45	10.69	15.54	13.24	13.65 ± 0.79
CsA-treated		Animal 1	Animal 2	Animal 3	Animal 4	Animal 5	Mean ± SEM
SRTM	BP_{ND}	10.01	11.01	10.11	10.19	12.48	10.76 ± 0.42
	R_I	0.763	0.686	0.744	0.601	0.759	0.711 ± 0.027
	k_2 (min^{-1})	0.278	0.256	0.302	0.302	0.317	0.291 ± 0.010
	k_2' (min^{-1})	0.364	0.373	0.405	0.502	0.417	0.412 ± 0.022
Logan	int′	−3111	−4244	−4057	−3338	−2951	−4263 ± 231
	DVR	12.99	15.19	15.07	14.06	14.55	14.38 ± 0.36
	BP_{ND}	11.99	14.19	14.07	13.06	13.55	13.38 ± 0.36

4. Discussion

Using two rodent models evidence was given that [^{18}F]FP is substrate of P-gp and this may have an impact on the brain uptake of this highly selective D_2/D_3 ligand. For the evaluation of a possible interaction between a compound and P-gp, different *in vitro* and *in vivo* methods are established. For *in vitro* examinations bidirectional transcellular transport assays are advantageous, since they allow for rapid screening of multiple drugs for their interaction with P-gp (Feng et al., 2008). However, these assays sometimes led to differing results, for example in the case of fluvoxamine (El Ela et al., 2004; Feng et al., 2008). Moreover, different groups may interpret similar results in a different manner, for example in the case of nortriptyline (Ejsing et al., 2006; Feng et al., 2008). In a recent *in vitro* study, various PET compounds were examined with

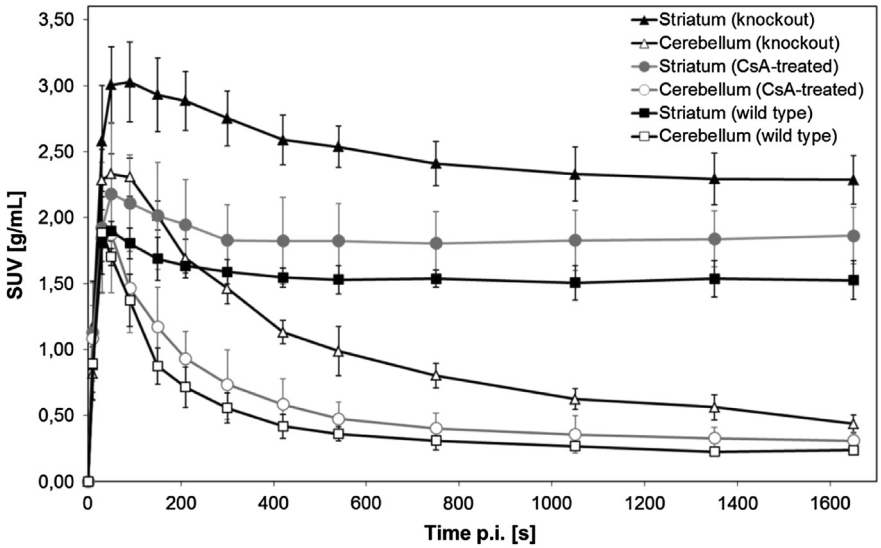

Fig. 4. Time activity curves from microPET-studies of [^{18}F]FP. Curves were drawn from activity measurements in striatum and cerebellum in wild type, CsA-treated and double knockout abcb1a/1b (−/−) FVB/N mice. Each curve gives the mean SUV±SD from 5 animals.

regard to possible substrate properties to P-gp, in which the authors reported that [^{18}F]FP was not a substrate in their assay (Tournier et al., 2011).

Due to the above mentioned considerations, possible interactions of [^{18}F]FP with P-gp were also examined in different *in vivo* studies. Since a P-gp-substrate is to some extent transported back to the plasma before it completely crosses the endothelial membrane, this effect can be either modeled by a decreased transport to brain, but also by an increased efflux from the brain (Liow et al., 2007). Thus, standard brain compartmental modeling with plasma time–activity curves cannot distinguish both possibilities, nor can it discriminate differing brain uptakes due to changes in receptor availability from those which are caused by P-gp interference. Furthermore, the blood levels of P-gp substrates are often also influenced by this efflux transporter, which further complicates a kinetic modeling based on blood TACs (Schinkel, 1999). In contrast, a reference tissue model, which uses the ratio of a receptor rich and a reference region for the calculation of the binding potential, is much less influenced by P-gp activity (Liow et al., 2007). Thus, if the P-gp activity is comparable in both, the receptor-rich and the reference region, reference tissue models should show the same BP_{ND} for wild type, pharmacologically modulated and knockout groups. Hence, in a first imaging study in Sprague Dawley rats the brain uptake in drug naive and P-gp-blocked animals was examined. Blocking of P-gp was performed using the immunosuppressive agent cyclosporine A, a potent P-gp inhibitor. This dose-dependent blocking was performed by intraperitoneal injection of 50 mg/kg of cyclosporine A, which has been proven an effective dose in a previous study (Schmitt et al., 2006). Since the i.p. injection resulted in a systemic availability of about 20% compared to an intravenous injection, this dose diminishes possible toxicological side effects of CsA, but allows an efficient blocking of P-gp, which however might not be 100% (Luke et al., 1990). CsA globally increased uptake of [^{18}F]FP into the brain, resulting in 45% and 48% higher radioactivity levels in the striatum and cerebellum, compared to the untreated group, indicating that [^{18}F]FP is indeed a substrate of P-gp in the rat model. This is further confirmed by the results of the kinetic modeling, since for both, the control and the CsA-treated group, equal values were obtained for k_2 and k_2'. Based on the assumption that P-gp only influences the tracer concentration in the tissue compartment and has no effect on other rate constants of the compartment model, the higher brain uptake of [^{18}F]FP in the CsA-treated group then only can be explained by a higher K_1, thus a higher influx rate constant.

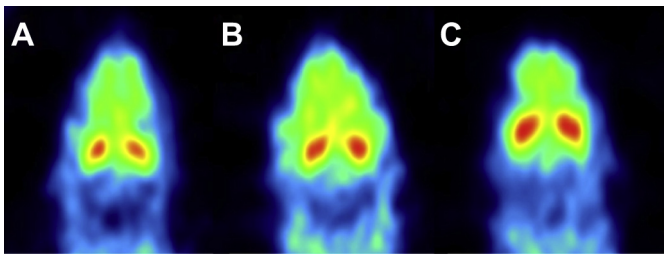

Fig. 5. Color coded uptake images. Coronal slices of the brain uptake of [^{18}F]FP in wild type (A), CsA-treated (B) and double knockout (C) FVB/N mice. The uptake is shown as averaged SUV from 20 to 30 min p.i., with a normalized color code (0–2 g/mL) for all images.

Furthermore, the kinetic modeling was also performed, to examine if CsA-treatment has an effect on binding potentials which were determined with a reference tissue model. In the simplified reference tissue models BP_{ND}s of 11.03 ± 0.63 and 10.76 ± 0.42 were calculated for the control and the CsA-treated group, whereas values of 13.65 ± 0.79 and 13.38 ± 0.36 were obtained in the noninvasive Logan plot. Hence, both models showed that the binding potentials are not influenced by P-glycoprotein in reference tissue models, indicating that the P-gp activity seems to be similar in striatum and cerebellum. The different values of the binding potentials for both models can be explained by the fact that, in contradiction to the SRTM, for the Logan plot only the last 20 min were used for the fitting, thus giving higher BP_{ND}s.

Since cyclosporine A is not only an inhibitor of P-gp, but also of CYP3A4 (Foxwell et al., 1989; Wacher et al., 1998), one of the most important enzymes for the metabolism of xenobiotics, the P-gp influence on the [^{18}F]FP uptake was also examined in a double knockout mouse model, thus avoiding influences possibly caused by drug metabolism. In contradiction to humans, where P-gp is encoded by a single gene (ABCB1), its function in rodents is performed by two different gene products: abcb1a and abcb1b (Devault and Gros, 1990). Nevertheless, P-gp shows a similar

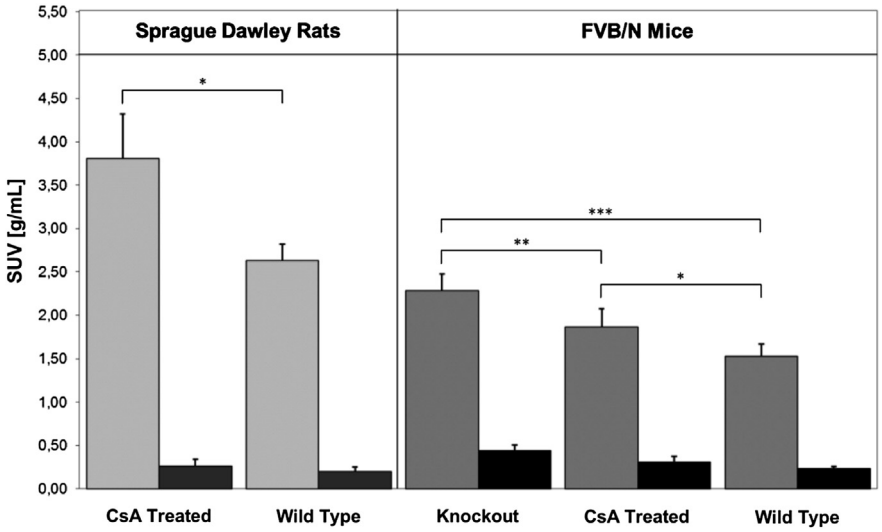

Fig. 6. Brain uptake comparisons. Comparison of the brain uptake of [^{18}F]FP in striatum (gray) and cerebellum (black) in CsA-treated and wild type Sprague Dawley (SD) rats after 60 min p.i. and double knockout, CsA-treated and wild type FVB/N mice after 30 min p.i. Given were means ± SEM, $^{*}p \leq 0.05$, $^{**}p \leq 0.01$, $^{***}p \leq 0.001$ by unpaired *t*-test.

distribution pattern in the tissue and similar substrate specificities for both species, making the double knockout mouse an important model for P-gp related *in vivo* studies (Ebinger and Uhr, 2006; Feng et al., 2008). For this reason, the imaging studies in the mouse model were not only performed in wild type and CsA-treated animals, but also in double knockout abcb1a/1b (−/−) FVB/N mice (Schinkel et al., 1997). In this imaging series the highest [^{18}F]FP uptakes were observed in the double knockout model, showing an increase (15–30 min p.i.) of 50% and 125% in the striatum and cerebellum compared to the untreated wild type animals. A possible explanation for the high percentage increase in the cerebellum is that the higher global brain uptake of [^{18}F]FP in the knockout model (cf. Fig. 4) produces some spillover effects from surrounding areas into the cerebellum, adding some uncertainty to these SUVs. In the CsA-treated FVB/N mice an increased uptake (15–30 min p.i.) of 20% and 35% for striatum and cerebellum was observed, which is remarkably lower compared to the KO model. These different SUVs between the knockout and the CsA-treated group can at best be explained by an incomplete blocking of the P-gp transporters by the injected dose of cyclosporine A or species specific differences in biodistribution kinetics resulting in different delays of brain peak concentrations (Luke et al., 1990). Hence, the imaging studies in FVB/N mice further indicate that [^{18}F]FP is a substrate of P-gp and that the higher uptake in the CsA-treated mice and rats is not an effect of the inhibition of CYP3A4 by cyclosporine A.

An overview of the obtained brain uptakes of [^{18}F]FP in Sprague Dawley rats and FVB/N mice at 60 and 30 min p.i. in wild type, CsA-treated and in the knockout model is shown in Fig. 6. The general lower SUVs in the mouse model in the striatum can be explained at least partial by increased partial volume effects in the mouse model, due to the much smaller mouse striatum compared to the rat striatum.

5. Conclusions

In conclusion, the possible influence of P-gp on the brain uptake of [^{18}F]FP was examined in microPET imaging studies in a rat (Sprague Dawley) and a mouse (FVB/N) model. In both experimental series, the CsA-treated or additionally knockout animals showed an increased brain uptake compared to the drug naïve control animals, indicating that [^{18}F]FP is a substrate of P-gp and its uptake is modulated by this efflux transporter. Since [^{18}F]FP is an important clinical D_2/D_3 radiotracer to examine striatal and extrastriatal dopamine concentrations in neuropsychiatric disorders or during pharmacological challenges, these results may appear relevant to further PET studies utilizing [^{18}F]FP. Moreover, P-gp genotyping of the examined subjects could be a helpful tool to determine the bioavailability of [^{18}F]FP, to avoid misinterpretations of obtained uptake values of this tracer.

Although several widely used antipsychotic drugs such as risperidone are substrates of P-gp, its exact role for the modulation of antipsychotic and adverse effects remains to be established. At least the incidence of adverse events seems to be dependent on the P-gp genotype (Jovanović et al., 2010). [^{18}F]FP is widely used for assessment of $D_{2/3}$ receptor occupancy by antipsychotic drugs, thus P-gp substrate properties of antipsychotic medication might influence PET results, too (Uhr et al., 2008; Holthoever et al., 2010). Albeit our study suggests that occupancy values are not influenced by the activity of P-gp using a reference tissue model for kinetic analysis, because the binding potential remains unchanged during treatment with cyclosporine A. It is therefore of utmost importance to confirm this suggestion in humans treated with antipsychotic drugs.

Acknowledgments

We thank Jan Timpe for his assistance in the production of [^{18}F]FP. Part of this research work was supported by a grant of the German Research Foundation (Grant Hi 399/6-1).

References

Aller, S.G., Yu, J., Ward, A., Weng, Y., Chittaboina, S., Zhuo, R., Harrell, P.M., Trinh, Y.T., Zhang, Q., Urbatsch, I.L., Chang, G., 2009. Structure of p-glycoprotein reveals a molecular basis for poly-specific drug binding. Science 323, 1718–1722.

Andersson, C., Hamer, R.M., Lawler, C.P., Mailman, R.B., Lieberman, J.A., 2002. Striatal volume changes in the rat following long-term administration of typical and atypical antipsychotic drugs. Neuropsychopharmacology 27, 143–151.

Bartels, A.L., Willemsen, A.T., Kortekaas, R., de Jong, B.M., de Vries, R., de Klerk, O., van Oostrom, J.C., Portman, A., Leenders, K.L., 2008. Decreased blood–brain barrier P-glycoprotein function in the progression of Parkinson's disease, PSP and MSA. J. Neural Transm. 115, 1001–1009.

Bozina, N., Kuzman, M.R., Medved, V., Jovanovic, N., Sertic, J., Hotujac, L., 2008. Associations between MDR1 gene polymorphisms and schizophrenia and

therapeutic response to olanzapine in female schizophrenic patients. J. Psych. Res. 42, 89–97.
Colabufo, N.A., Berardi, F., Perrone, M.G., Capparelli, E., Cantore, M., Inglese, C., Perrone, R., 2010. Substrates, inhibitors and activators of p-glycoprotein: candidates for radiolabeling and imaging perspectives. Curr. Top. Med. Chem. 10, 1703–1714.
Constantinescu, C.C., Coleman, R.A., Pan, M.-L., Mukherjee, M., 2011. Striatal and extrastriatal MicroPET imaging of D_2/D_3 dopamine receptors in rat brain with [^{18}F]Fallypride and [^{18}F]Desmethoxyfallypride. Synapse 65, 778–787.
Cordon-Cardo, C., O'Brien, J.P., Casals, D., Rittman-Grauer, L., Biedler, J.L., Melamed, M.R., Bertino, J.R., 1989. Multidrug–resistance gene (P-glycoprotein) is expressed by endothelial cells at blood-brain barrier sites. Proc. Natl. Acad. Sci. U. S. A. 86, 695–698.
Devault, A., Gros, P., 1990. Two members of the mouse mdr gene family confer multidrug resistance with overlapping but distinct drug specificities. Mol. Cell Biol. 10, 1652–1663.
Dutheil, F., Dauchy, S., Diry, M., Sazdovitch, V., Cloarec, O., Mellottée, L., Bièche, I., Ingelman-Sundberg, M., Flinois, J.P., de Waziers, I., Beaune, P., Declèves, X., Duyckaerts, C., Loriot, M.A., 2009. Xenobiotic-metabolizing enzymes and transporters in the normal human brain: regional and cellular mapping as a basis for putative roles in cerebral function. Drug Metab. Dispos. 37, 165–174.
Ebinger, M., Uhr, M., 2006. ABC drug transporter at the blood-brain barrier – effects on drug metabolism and drug response. Eur. Arch. Psy. Clin. N. 256, 294–298.
Ejsing, T.B., Hasselstrom, J., Linnet, K., 2006. The influence of P-glycoprotein on cerebral and hepatic concentrations of nortriptyline and its metabolites. Drug Metab. Drug Interact. 21, 139–162.
El Ela, A.A., Hartter, S., Schmitt, U., Hiemke, C., Spahn-Langguth, H., Langguth, P., 2004. Identification of P-glycoprotein substrates and inhibitors among psychoactive compounds – implications for pharmacokinetics for selected substrates. J. Pharm. Pharmacol. 56, 967–975.
Elsinga, P.H., Hendrikse, N.H., Bart, J., van Waarde, A., Vaalburg, W., 2005. Positron Emission Tomography studies on binding of central nervous system drugs and P-glycoprotein function in the rodent brain. Mol. Imaging Biol. 7, 37–44.
Feng, B., Mills, J.B., Davidson, R.E., Mireles, R.J., Janiszewski, J.S., Troutman, M.D., de Morais, S.M., 2008. In-vitro P-glycoprotein assays to predict the in vivo interactions of P-glycoprotein with drugs in the central nervous system. Drug Metab. Dispos. 36, 268–275.
Foxwell, B.M., Mackie, A., Ling, V., Ryffel, B., 1989. Identification of the multidrug resistance-related P-glycoprotein as a cyclosporine binding protein. Mol. Pharmacol. 36, 543–546.
Gründer, G., Siessmeier, T., Piel, M., Vernaleken, I., Buchholz, H.G., Zhou, Y., Hiemke, C., Wong, D.F., Rösch, F., Bartenstein, P., 2003. Quantification of D_2-like dopamine receptors in the human brain with ^{18}F-Desmethoxyfallypride. J. Nucl. Med. 44, 109–116.
Gunn, R.N., Lammertsma, A.A., Hume, S.P., Cunningham, V.J., 1997. Parametric imaging of ligand-receptor binding in PET using a simplified reference region model. Neuroimage 6, 279–287.
Holthoever, D., Hiemke, C., Schmitt, U., 2010. Induction of drug transporters alters disposition of risperidone – a study in mice. Pharmaceutics 2, 258–274.
Ishiwata, K., Kawamura, K., Yanai, K., Yanai, K., Hendrikse, N.H., 2007. In vivo evaluation of p-glycoprotein modulation of 8 PET radioligands used clinically. J. Nucl. Med. 48, 81–87.
Jovanović, N., Božina, N., Lovrić, M., Medved, V., Jakovljevic, M., Peles, A.M., 2010. The role of CYP2D6 and ABCB1 pharmacogenetics in drug-naïve patients with first-episode schizophrenia treated with risperidone. Eur. J. Clin. Pharmacol. 66, 1109–1117.
Juliano, R.L., Ling, V., 1976. A surface glycoprotein modulating drug permeability in Chinese hamster ovary cell mutants. Biochim. Biophys. Acta 455, 152–162.
Liow, J.S., Lu, S., McCarron, J.A., Hong, J., Musachio, J.L., Pike, V.W., Innis, R.B., Zoghbi, S.S., 2007. Effect of a p-glycoprotein inhibitor, cyclosporin a, on the disposition in rodent brain and blood of the 5-HT_{1A} receptor radioligand, [^{11}C](R)-(—)-RWAY. Synapse 61, 96–105.
Logan, J., Fowler, J.S., Volkow, N.D., Ding, Y.-S., Alexoff, D.L., 1996. Distribution volume ratios without blood sampling from graphical analysis of PET data. J. Cereb. Blood Flow Metab. 16, 834–840.
Luke, D.R., Brunner, L.J., Vadiei, K., 1990. Bioavailability assessment of cyclosporine in the rat. Influence of route administration. Drug Metab. Dispos. 18, 158–162.
Martin, C., Berridge, G., Mistry, P., Higgins, C., Charlton, P., Callaghan, R., 2000. Drug binding sites on P-glycoprotein are altered by ATP binding prior to nucleotide hydrolysis. Biochem 39, 11901–11906.
Mukherjee, J., Yang, Z.Y., Das, M.K., Brown, T., 1995. Fluorinated benzamide neuroleptics – III. Development of (S)-N-[(1-allyl-2-pyrrolidinyl)methyl]-5-(3-[^{18}F] fluoropropyl)-2,3-dimethoxybenzamide as an Improved Dopamine D-2 Receptor Tracer. Nucl. Med. Biol. 22, 283–296.
Ohtsuki, S., Terasaki, T., 2007. Contribution of carrier-mediated transport systems to the blood-brain barrier as a supporting and protecting interface for the brain; importance for CNS drug discovery and development. Pharm. Res. 24, 1745–1758.
Pardridge, W.M., 2007. Blood-brain barrier delivery. Drug Disc. Today 12, 54–61.
Paxinos, G., Watson, C., 2007. The Rat Brain in Stereotaxic Coordinates, sixth ed. Academic Press, London.
Schinkel, A.H., Mayer, U., Wagenaar, E., Mol, C.A., van Deemter, L., Smit, J.J., van der Valk, M.A., Voordouw, A.C., Spits, H., van Tellingen, O., Zijlmans, J.M., Fibbe, W.E., Borst, P., 1997. Normal viability and altered pharmacokinetics in mice lacking mdr1-type (drug-transporting) P-glycoproteins. Prog. Natl. Acad. Sci. U. S. A. 94, 4028–4033.
Schinkel, A.H., 1999. P-Glycoprotein, a gatekeeper in the blood–brain barrier. Adv. Drug Del. Rev. 36, 179–194.
Schmitt, U., Abou El-Ela, A., Guo, L.J., Glavinas, H., Krajcsi, P., Baron, J.M., Tillmann, C., Hiemke, C., Langguth, P., Härtter, S., 2006. Cyclosporine A (CsA) affects the pharmacokinetics of the atypical antipsychotic amisulpride probably via inhibition of P-glycoprotein (P-gp). J. Neural Transm. 113, 787–801.
Siessmeier, T., Zhou, Y., Buchholz, H.G., Landvogt, C., Vernaleken, I., Piel, M., Schirrmacher, R., Rösch, F., Schreckenberger, M., Wong, D.F., Cumming, P., Gründer, G., Bartenstein, P., 2005. Parametric mapping of binding in human brain of d_2 receptor ligands of different affinities. J. Nucl. Med. 46, 964–972.
Slow, E.J., van Raamsdonk, J., Rogers, D., Coleman, S.H., Graham, R.K., Deng, Y., Oh, R., Bissada, N., Hossain, S.M., Yang, Y.-Z., Li, X.-J., Simpson, E.M., Gutekunst, C.-A., Leavitt, B.R., Hayden, M.R., 2003. Selective striatal neuronal loss in a YAC128 mouse model of huntington disease. Hum. Mol. Gen. 12, 1555–1567.
Tournier, N., Valette, H., Peyronneau, M.A., Saba, W., Goutal, S., Kuhnast, B., Dollé, F., Scherrmann, J.M., Cisternino, S., Bottlaender, M., 2011. Transport of selected PET radiotracers by human p-glycoprotein (ABCB1) and breast cancer resistance protein (ABCG2): an in vitro screening. J. Nucl. Med. 52, 415–423.
Uhr, M., Tontsch, A., Namendorf, C., Ripke, S., Lucae, S., Ising, M., Dose, T., Ebinger, M., Rosenhagen, M., Kohli, M., Kloiber, S., Salyakina, D., Bettecken, T., Specht, M., Pütz, B., Binder, E.B., Müller-Myhsok, B., Holsboer, F., 2008. Polymorphisms in the drug transporter gene ABCB1 predict antidepressant treatment response in depression. Neuron 57, 203–209.
Vernaleken, I., Peters, L., Raptis, M., Lin, R., Buchholz, H.G., Zhou, Y., Winz, O., Rösch, F., Bartenstein, P., Wong, D.F., Schäfer, W.M., Gründer, G., 2011. The applicability of SRTM in [^{18}F]fallypride PET investigations: impact of scan durations. J. Cereb. Blood Flow. Metab. 31, 1958–1966.
Wacher, V.J., Silverman, J.A., Zhang, Y., Benet, L.Z., 1998. Role P-glycoprotein and cytochrome P450 3A in limiting oral absorption of peptides and peptidomimetics. J. Pharm. Sci. 87, 1322–1330.